New Phytologist

Research

AtSERPIN1 is an inhibitor of the metacaspase AtMC1-mediated cell death and autocatalytic processing *in planta*

Saul Lema Asqui[1], Dominique Vercammen[2,3], Irene Serrano[4], Marc Valls[5], Susana Rivas[4], Frank Van Breusegem[2,3,6,7], Frank L. Conlon[8,9,10,11], Jeffery L. Dangl[12,13,14,15,16] and Núria S. Coll[1]

[1]Centre for Research in Agricultural Genomics (CRAG), CSIC-IRTA-UAB-UB, Campus UAB, Bellaterra, Barcelona 08193, Spain; [2]Department of Plant Systems Biology, VIB, Ghent 9052, Belgium; [3]Department of Plant Biotechnology and Bioinformatics, Ghent University, Ghent 9052, Belgium; [4]LIPM, Université de Toulouse, INRA, CNRS, Castanet-Tolosan, France; [5]Department of Genetics, Universitat de Barcelona and Centre for Research in Agricultural Genomics (CSIC-IRTA-UAB-UB) Edifici CRAG, Campus UAB, Bellaterra, Catalonia 08193, Spain; [6]Department of Medical Protein Research, VIB, Ghent 9000, Belgium; [7]Department of Biochemistry, Ghent University, Ghent 9000, Belgium; [8]Department of Biology, University of North Carolina, Chapel Hill, NC 27599, USA; [9]Department of Genetics, University of North Carolina, Chapel Hill, NC 27599, USA; [10]McAllister Heart Institute, University of North Carolina, Chapel Hill, NC 27599, USA; [11]Lineberger Cancer Center, University of North Carolina, Chapel Hill, NC 27599, USA; [12]Department of Biology, University of North Carolina, Chapel Hill, NC 27599-3280, USA; [13]Howard Hughes Medical Institute, University of North Carolina, Chapel Hill, NC 27599-3280, USA; [14]Curriculum in Genetics and Molecular Biology, University of North Carolina, Chapel Hill, NC 27599-3280, USA; [15]Carolina Center for Genome Sciences, University of North Carolina, Chapel Hill, NC 27599-3280, USA; [16]Department of Microbiology and Immunology, University of North Carolina, Chapel Hill, NC 27599-3280, USA

Author for correspondence:
Nuria S. Coll
Tel: +34 93 5606600
Email: nuria.sanchez-coll@cragenomica.es

Received: *20 June 2016*
Accepted: *16 December 2016*

New Phytologist (2017)
doi: 10.1111/nph.14446

Key words: hypersensitive response (HR), metacaspase, plant–pathogen interactions, programmed cell death, protease, serpin.

Summary

- The hypersensitive response (HR) is a localized programmed cell death phenomenon that occurs in response to pathogen recognition at the site of attempted invasion. Despite more than a century of research on HR, little is known about how it is so tightly regulated and how it can be contained spatially to a few cells.
- AtMC1 is an *Arabidopsis thaliana* plant metacaspase that positively regulates the HR. Here, we used an unbiased approach to identify new AtMC1 regulators. Immunoaffinity purification of AtMC1-containing complexes led us to the identification of the protease inhibitor AtSerpin1.
- Our data clearly showed that coimmunoprecipitation between AtMC1 and AtSerpin1 and formation of a complex between them was lost upon mutation of the AtMC1 catalytic site, and that the AtMC1 prodomain was not required for the interaction. AtSerpin1 blocked AtMC1 self-processing and inhibited AtMC1-mediated cell death. Our results constitute an *in vivo* example of a Serpin acting as a suicide inhibitor in plants, reminiscent of the activity of animal or viral serpins on immune/cell death regulators, including caspase-1.
- These results indicate a conserved function of a protease inhibitor on cell death regulators from different kingdoms with unrelated modes of action (i.e. caspases vs metacaspases).

Introduction

Metacaspases are a family of proteases present in plants, fungi and protozoa (Uren *et al.*, 2000). They are members of the clan CD of cysteine proteases, featuring a unique tertiary structure termed the caspase-hemoglobinase fold that encloses a conserved cysteine–histidine catalytic dyad (Aravind & Koonin, 2002). Members of this superfamily also include caspases, animal cysteine proteases with aspartate specificity that have essential roles in inflammation and cell death. Metacaspases have typically been compared with caspases, but research has shown that despite their overall active site configuration, their mode of action might be radically different. First, they have different substrate sequence cleavage requirements: lysine or arginine for metacaspases and aspartic acid for caspases; second, metacaspase activity is not blocked by caspase inhibitors; and third, according to their structure, metacaspases cannot form dimers the way caspases do (Salvesen *et al.*, 2016). Regardless of these differences, metacaspases have been shown to act as cell death regulators (Coll *et al.*, 2010, 2014; Tsiatsiani *et al.*, 2011; Wrzaczek *et al.*, 2015), although it is not clear how they exert this function or how they are regulated.

Arabidopsis metacaspases are the best characterized among plants. The Arabidopsis genome encodes nine metacaspases, AtMC1–AtMC3 (type I) and AtMC4–AtMC9 (type II). The main difference between type I and type II metacaspases is the presence (type I)/absence (type II) of an N-terminal prodomain. According to the crystal structure of the Trypanosomas type I metacaspase (McLuskey *et al.*, 2012), the prodomain rests as a lid on top of the catalytic fold, presumably precluding substrate access until cleavage or a conformational change occurs. In agreement with that proposal, the prodomains of AtMC1 and AtMC2

were shown to negatively regulate their function (Coll *et al.*, 2010).

We previously demonstrated that AtMC1 is a positive regulator of pathogen-triggered hypersensitive response (HR) cell death (Coll *et al.*, 2010), a plant reaction that takes place locally at the site of attempted pathogen attack upon recognition of the invader. In this context, catalytic integrity was critical for AtMC1 cell death function. Conditional overexpression of AtMC1 resulted in ectopic cell death, which indicated that a tight regulation of this protein must be in place in order to prevent uncontrolled cell death. So far, two negative regulators of AtMC1 have been identified: AtMC2 and the negative regulator of plant defense and HR, LSD1 (Dietrich *et al.*, 1994). AtMC1 interacted with LSD1 through its prodomain, whereas AtMC1 and AtMC2 did not interact with each other and the details of their interplay remain to be clarified (Coll *et al.*, 2010).

Here, we used an unbiased approach to identify new regulators of AtMC1 activity. Immunoaffinity purification of AtMC1-containing complexes led us to the identification of the protease inhibitor AtSerpin1. Our data clearly showed that coimmunoprecipitation between AtMC1 and AtSerpin1 was dependent on an intact AtMC1 catalytic site and the prodomain was not required for the interaction. Furthermore, AtSerpin1 blocked AtMC1 self-processing and inhibited AtMC1-mediated cell death. Together, our findings uncover AtSerpin1 as a bona fide AtMC1 inhibitor *in planta*.

Materials and Methods

Plant material and growth conditions

All experiments were performed using *Arabidopsis thaliana* (L.) Heynh.accession Col-0. Mutant *atmc1* and the transgenic *atmc1* P_{AtMC1}*::AtMC1-HA* and *lsd1 atmc1* P_{AtMC1}*::AtMC1-HA* were previously described in Coll *et al.* (2010). Mutant *atserpin1* and transgenic Col-0 *35S::AtSerpin1-HA* lines were described in Lampl *et al.* (2010). Arabidopsis was grown under short-day conditions (9 : 15 h, 22 : 20°C, light : dark).

Nicotiana benthamiana was grown under long-day conditions (16 : 8 h, 25 : 22°C, light : dark).

DNA constructs

To obtain the P_{AtMC1}*::HA-AtMC1* construct, the product of an overlapping PCR using *AtMC1* promoter and HA-AtMC1 was directionally cloned into pENTR/D/TOPO Gateway vector (Invitrogen) and recombined into the plant binary Gateway-compatible vector pGWB1 (Nakagawa *et al.*, 2007).

The AtSerpin1 full-length cDNA was directionally cloned into pENTR/D/TOPO Gateway vector (Invitrogen) and recombined into the plant binary Gateway-compatible vector pGWB641 to obtain *35S::AtSerpin1-YFP* or pGWB642 to obtain *35S::YFP-AtSerpin1* (Nakamura *et al.*, 2010).

For subcellular localization experiments, fusion of fluorescent proteins to AtMC1, AtMC1-ΔN, AtMC1-CA and AtSerpin1 was performed using a multisite GATEWAY cloning strategy (Invitrogen) described previously (Gu & Innes, 2011). Briefly, the full-length open reading frames of *AtMC1*, *AtMC1-ΔN*, *AtMC1-CA* and *AtSerpin1* were cloned into the donor vector pBSDONR P1-P4 (an ampicillin-resistant vector derived from pDONR221 P1-P4 from Invitrogen) (Gu & Innes, 2011) using the BP cloning Kit (Invitrogen). C-terminal eGFP (Cormack *et al.*, 1996) and C-terminal red fluorescent protein (RFP) (Campbell *et al.*, 2002) were cloned into the entry vector pBSDONR P4r-P2. To fuse AtMC1, AtMC1-ΔN, AtMC1-CA and AtSerpin1 with the epitope tags, the P1–P4 clones were recombined with corresponding P4r-P2 and the desired destination vectors using Gateway LR clonase II (Invitrogen). For AtMC1, AtMC1-ΔN, and AtMC1-CA, the earlier described pBSDONR constructs were recombined with the destination vector pEarleyGate100 (Earley *et al.*, 2006). For AtSerpin1, the corresponding pBSDONR constructs were recombined with the steroid-inducible destination vector pBAV154 (Vinatzer *et al.*, 2006).

Plasmids were transformed into *Agrobacterium tumefaciens* strain GV3101 (pMP90) by electroporation and plated into selective Luria-Bertani (LB) agar plates.

Stable transformation of *Arabidopsis thaliana*

atmc1 P_{AtMC1}*::AtMC1-HA* plants were transformed with *35S::AtSerpin1-YFP* using *Agrobacterium tumefaciens* (GV3101)-mediated floral dip as previously described (Clough & Bent, 1998). Homozygous double transgenic lines were selected on Murashige & Skoog (MS) media supplemented with 20 μg ml^{-1} Basta (glufosinate-ammonium). *atmc1* plants were transformed with P_{AtMC1}*::HA-AtMC1* using *A. tumefaciens* (GV3101)-mediated floral dip as previously described (Clough & Bent, 1998). Homozygous transgenic lines were selected on MS media supplemented with 50 μg ml^{-1} hygromycin.

Immunoisolation of protein complexes from *Arabidopsis*

Homozygous *atmc1* or *lsd1 atmc1* P_{AtMC1}*::AtMC1-HA* were used for immunoaffinity purification 24 h after spraying them with 300 μM BTH as previously described (Coll *et al.*, 2010). All materials and reagents for immunoisolation were from Thermo Fisher Scientific (Waltham, MA, USA), unless otherwise stated. AtMC1–HA complexes were immunoisolated using magnetic beads (M-270 epoxy Dynabeads) conjugated to a monoclonal HA antibody (MMS-101P MONO HA.11; Covance, Princeton, NJ, USA). For conjugation, 100 μg of antibody were first washed and concentrated to the final volume of 100 μl by three rounds of adding 500 μl of phosphate-buffered saline and centrifugation at 9000 ***g*** for 15 min at 4°C using a centrifugal filter (Amicon; Merck Millipore, Billerica, MA, USA). One hundred micrograms (100 μl) of clean antibody were added to 18 mg of magnetic beads washed with 0.1 M sodium phosphate buffer (pH 7.4). Then, 120 μl of 3 M ammonium sulfate and 120 μl of 0.1 M sodium phosphate buffer (pH 7.4) were added. Beads were incubated overnight at 30°C on an orbital shaker. In parallel, 10 g of leaves

were snap-frozen in liquid nitrogen and cryogenically lysed using a Retsch MM 301 Mixer Mill (20 cycles of 180 s at 30 Hz) (Retsch, Newtown, PA, USA). The frozen powder was resuspended in cold lysis buffer (20 mM K-HEPES pH 7.4, 110 mM CH_3CO_2K, 2 mM $MgCl_2$, 0.1% Tween-20, 1 μM $ZnCl_2$, 1 μM $CaCl_2$), supplemented with protease inhibitor cocktail (Roche). Lysates were homogenized using a polytron (two cycles of 15 s). The cell lysate was centrifuged at 1000 ***g*** at 4°C for 10 min. The supernatant was collected and filtered through a syringe-driven 5 μm filter to remove any particles from lysate that did not pellet. The protein concentration of the lysate was measured, to adjust all samples to the same concentration. A fraction of the lysate was reserved to run on a sodium dodecyl sulfate–polyacrylamide gel electrophoresis (SDS-PAGE) (total protein).

Beads were equilibrated by washing three times with lysis buffer. After that, 1 ml of lysate was added to the beads. Beads were then incubated at 4°C on an orbital shaker. After 1 h, tubes were placed on a Dynal (Thermo Fisher Scientific, Waltham, MA, USA) magnetic rack, flowthrough was discarded and beads were washed five times with lysis buffer. Forty microliters of elution buffer (4× NuPAGE LDS Sample Buffer and 20× NuPAGE Sample Reducing Buffer; Thermo Fisher Scientific) supplemented with 2 μl of 1 M iodoacetamide were added per sample and incubated 1 h at room temperature. Subsequently, samples were transferred to 70°C to elute proteins off the beads. Eluted proteins were partially separated at 150 V on a NuPAGE 3–12% 1-mm-thick Bis-Tris protein gel using NuPAGE MOPS running buffer, supplemented with NuPAGE Antioxidant in the inner gel chamber. The gel was stained using Coomassie SimplyBlue SafeStain (Thermo Fisher Scientific). Each lane was excised and divided in eight fragments. Fragments were individually analyzed by mass spectrometry.

Protein characterization using mass spectrometry

Excised SDS-PAGE gel bands were in-gel-digested with trypsin. The extracted peptides were separated on a nanoAcquity HPLC system (Waters Corp., Milford, MA, USA) with a 360 μm OD × 75 μm ID analytical column (14 cm of Magic 5 μm C18AQ resin; Michrom Biosciences, Bruker Corp., Billerica, MA, USA). The liquid chromatography (LC) system was directly connected through an electrospray ionization source interfaced to an LTQ Orbitrap Velos ion trap mass spectrometer (Thermo Fisher Scientific) controlled by Xcalibur software (v.2.1.0.1140; Thermo Fisher Scientific) and operated in the data-dependent mode in which the initial MS scan recorded the mass to charge (*m/z*) ratios of ions over the range 400–2000. Raw files were searched using Mascot (v.2.3.02; Matrix Science, Wyndham Place, UK). Search parameters included peptide mass tolerance of 10 ppm and fragment ion tolerance of 0.8 mass units.

Isolated protein complexes were analyzed by mass spectrometry as previously described (Kaltenbrun *et al.*, 2013). Briefly, tandem mass spectra were extracted by Proteome Discoverer (Thermo Fisher Scientific), and all MS/MS samples were analyzed with Sequest (v.1.2.0.208; Thermo Fisher Scientific), set up to search the Arabidopsis UniProt-SwissProt protein sequence database, assuming digestion pattern with trypsin. Scaffold (v. Scaffold_3_00_06; Proteome Software Inc., Portland, OR, USA) was used to validate MS/MS-based peptide and protein identifications. Peptide sequences were deemed a match if they could be established at > 95.0% probability as specified by the PeptideProphet algorithm (Keller *et al.*, 2002). In turn, protein identifications were deemed a match if they could be established at > 99.0% probability by the ProteinProphet algorithm and have at least one sequenced peptide.

The mass spectrometry proteomics data have been deposited to the ProteomeXchange Consortium via the PRIDE partner repository with the dataset identifier PXD005134 and 10.6019/PXD005134. The description of all files uploaded to ProteomeXchange can be found in Supporting Information Table S1.

Transient protein expression in *N. benthamiana*

Transient *A. tumefaciens*-mediated transformation of *N. benthamiana* leaves was performed as previously described (Coll *et al.*, 2010). Whole *N. benthamiana* leaves (*c.* 500 mg each) transiently expressing the constructs to test together with the anti-silencing vector p19 (Voinnet *et al.*, 2003) – Dex::AtMC1-HA + 35S::p19 (OD_{600} 0.2 + 0.1), Dex::AtMC1-HA + 35S::AtSerpin1 + 35S::p19 (OD_{600} 0.2 + 0.4 + 0.1), Dex::AtMC1-ΔN-HA + 35S::p19 (OD_{600} 0.4 + 0.1), Dex::AtMC1-ΔN-HA + 35S::AtSerpin1 + 35S::p19 (OD_{600} 0.4 + 0.4 + 0.1), Dex::AtMC1-CA-HA + 35S::p19 (OD_{600} 0.2 + 0.1), Dex::AtMC1-CA-HA + 35S::AtSerpin1 + 35S::p19 (OD_{600} 0.2 + 0.4 + 0.1), 35S::AtSerpin1 + 35S::p19 (OD_{600} 0.4 + 0.1) – were frozen in liquid nitrogen before further processing for protein extraction.

Colocalization experiment

Agrobacterium tumefaciens cultures carrying the indicated constructs were grown and resuspended in water at $OD_{600} = 0.8$ (Wroblewski *et al.*, 2005). For coexpression of multiple constructs, suspensions were mixed in equal ratios. Bacterial suspension mixtures were infiltrated using a needleless syringe. Samples were collected for microscopic imaging 40 h after infiltration.

Confocal laser scanning microscopy

Confocal laser scanning microscopy was performed on a Leica SP2 AOBS inverted confocal microscope (Leica Microsystems, Wetzlar, Germany) equipped with a ×40, numerical aperture-1.2 water objective. eGFP fusion was excited with a 488 nm Argon laser and detected using a 505–530 bandpass emission filter. RFP fusions were excited using a 561 nm He-Ne laser and detected using a custom 595–620 nm bandpass emission filter.

Coimmunoprecipitation assays and protein analysis

Frozen samples were ground using a mortar and pestle on 3 ml of lysis buffer (200 mM K-HEPES pH 7.4, 1.1 M C_2H_3KO, 20 mM $MgCl_2$, 1% Tween-20, 10 μM $ZnCl_2$, 10 μM $CaCl_2$),

supplemented with 5 mM dithiothreitol (DTT), and protease inhibitor cocktail (Roche). Homogenized samples were filtered through miracloth (Millipore) and collected in 15 ml tubes. Samples were then centrifuged for 15 min at 4°C and 7000 ***g*** to separate the cell debris from the total protein extract.

For coimmunoprecipitation, total protein extracts were diluted to 2 mg ml^{-1} and incubated with 50 µl of anti green fluorescent protein (GFP) magnetic beads (MACS; Miltenyi Biotec, Bergisch, Gladbach, Germany), for 2 h at 4°C under constant rotation. Bound proteins were eluted according to the manufacturer's instructions. Twenty-five micrograms of total protein (input), an equal volume of flowthrough (unbound) and 20 µl of eluate were loaded onto an SDS-PAGE gel. Immunoblots were performed using 1 : 5000 anti-GFP mouse monoclonal antibody (clone B-2; Santa Cruz Biotechnology, Dallas, TX, USA) or 1 : 5000 monoclonal anti-HA-HRP (clone 3F10; Roche).

To test binding between AtMC1 and AtSerpin1, we followed the protocol established by Roberts *et al.* (2011). In essence, protein extraction was performed using a Laemmli buffer (120 mM Tris-HCl pH 6.8, 4% SDS (w/v), 15% glycerol (v/v), 0,02% bromophenol (w/v)) with or without DTT (5 mM) as reducing agent. Proteins were then separated on 10% or 7.5% SDS-PAGE gels and probed with 1 : 5000 monoclonal anti-HA-HRP (clone 3F10; Roche) or 1 : 5000 anti-GFP mouse monoclonal antibody (clone B-2; Santa Cruz Biotechnology).

Chemical treatments

Dexamethasone was applied to *N. benthamiana* leaf surfaces using cottonballs to induce expression of *AtMC1* forms under the control of the dexamethasone promoter (Coll *et al.*, 2010) 48 h after agroinfiltration. Leaves were treated with 0.2 µM dexamethasone and samples were collected 24 h later.

Three-week-old Arabidopsis plants were sprayed with 150 µM benzol(1,2,3)thiadiazole-7-carbothioic acid S-methyl ester.

The proteasome inhibitor MG-132 (2 µM in 0.2% dimethyl sulfoxide; Sigma-Aldrich) was applied on *N. benthamiana* leaf surfaces 24 h after dexamethasone treatment and samples were collected 12 h later.

Cell death analyses

Ion leakage assays were carried out using 3-wk-old *N. benthamiana* plants transiently expressing different protein combinations (see the 'Transient protein expression in *N. benthamiana*' subsection earlier). At least four leaves per combination were used. Fifteen disks were extracted per leaf with a cork borer (7 mm diameter) and placed on a plate with distilled water during 1 h. After that, 10 disks were placed in a flask containing 10 ml of distilled water (six replicates per sample). Conductivity was measured over time using a hand electrical conductivitymeter (FG3-FIVEGO, Schwerzenbach, Switzerland).

Trypan blue staining of *N. benthamiana* leaves was performed by collecting whole leaves in 50 ml tubes (each leaf in a separate tube) 72 h after cell death induction and covered with a total of 35 ml of a 1 : 3 dilution of trypan blue stock solution (Keogh *et al.*, 1980). The tubes were incubated in previously boiled water for 15 min, and then cleared overnight with chloral hydrate on an orbital shaker. Pictures were taken 72 h after cell death induction. Pictures were also processed adding a binary mask using ImageJ (v.1.50i; National Institues of Health, Bethesda, MD, USA).

Arabidopsis single cell death assay was performed according to Coll *et al.* (2010).

Results

Two forms of AtMC1 coexist in plants: full length and a prodomain-less

We previously showed that removal of AtMC1 prodomain enhances its pro-death activity in Arabidopsis (Coll *et al.*, 2010). To determine whether prodomain removal occurs in nature, we compared the processing pattern of N-terminally vs C-terminally tagged protein from transgenic plants expressing *HA-AtMC1* or *AtMC1-HA* under the control of AtMC1 promoter (P_{AtMC1}*::HA-AtMC1* or P_{AtMC1}*::AtMC1-HA*, respectively) (Fig. S1). Immunoblot using an anti-HA antibody clearly showed that AtMC1-HA is present in both its full-length form (41 kDa) and a fragment of *c.* 36 kDa, presumably corresponding to an autoprocessed form (Fig. 1). By contrast, in plants expressing HA-AtMC1 only the full-length form of the protein could be detected by anti-HA immunoblot. This supports the idea that the spontaneously formed smaller AtMC1 fragment corresponds to the prodomain-less version of the protein, indicative of N-terminal processing.

Immunoaffinity isolation identified the protease inhibitor AtSerpin1 as part of AtMC1-containing protein complexes

In order to identify regulators of AtMC1 activity under native conditions, we performed immunoaffinity purification of AtMC1-containing complexes using rosette leaves from 4-wk-old *atmc1* plants expressing AtMC1 under the control of its own promoter (*atmc1* P_{AtMC1}*::AtMC1-HA*, Fig. S1). Immunopurified proteins were partially resolved using SDS-PAGE (Fig. S2) and in-gel-digested with trypsin. Analysis was performed using nLC-

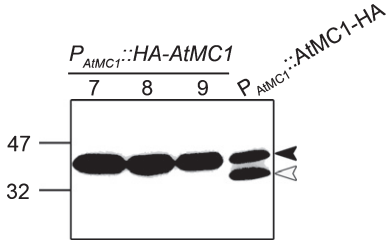

Fig. 1 The prodomain of the metacaspase *Arabidopsis thaliana* AtMC1 is cleaved in plants. Immunoblot using anti-HA antibodies of three independent *atmc1* P_{AtMC1}*::HA-AtMC1* T_1 lines (7–9) compared with homozygous *atmc1* P_{AtMC1}*::HA-AtMC1*. Black and white arrows indicate full-length and cleaved AtMC1, respectively.

tandem MS (MS/MS) on an LTQ Orbitrap Velos. Two independent biological replicates were performed. Raw MS/MS spectra were first analyzed by SEQUEST database searches (PROTEOME DISCOVERER) and loaded into SCAFFOLD for further analysis. Protein identifications from all replicates were filtered using stringent confidence parameters (see the Materials and Methods section). Through this analysis we detected 154–1300 proteins per condition, among which we identified the protease inhibitor AtSerpin1. AtSerpin1 was not identified in the experimental controls used (Table S2).

AtSerpin1 inhibits AtMC1 autoprocessing *in vivo*

Conditional overexpression of *AtMC1* in *N. benthamiana* leaves resulted in accumulation of both full-length and processed forms similar to when expressed in Arabidopsis under the control of its native promoter (Fig. S3). AtMC1 cleavage was inhibited by mutation of the predicted catalytic site (Fig. 2b, AtMC1-CA), indicative of autoprocessing. AtSerpin1 coexpression with AtMC1 also blocked autocatalytic processing of AtMC1 (Figs 2a, S3). Absence of processed AtMC1 is consistent with the idea that AtSerpin1 acts as an inhibitor of AtMC1 cleavage *in planta*.

Interestingly, AtSerpin1 caused a sharp decrease in the levels of AtMC1-CA (Fig. 2b). To explain this observation, we hypothesized that AtSerpin1 might bind and/or alter the structure of the AtMC1 catalytic mutant, ultimately leading to its proteasomal degradation. To test whether the reduction in AtMC1-CA protein levels caused by AtSerpin1 coexpression was proteasome-dependent, we treated agroinfiltrated *N. benthamiana* leaves with the proteasome inhibitor MG-132 or left them untreated. As shown in Fig. 2(b) the severe reduction of AtMC1-CA levels caused by *AtSerpin1* coexpression could be totally reverted by proteasome inhibition. However, the AtSerpin1-dependent degradation of AtMC1-CA might partly occur during protein extraction as a result of the reducing conditions caused by DTT. The data also indicated that, when expressed alone, AtMC1-CA is also partly degraded by the proteasome, as the levels increase after MG-132 treatment when compared with untreated leaves. By contrast, the native full-length and processed forms of AtMC1 do not seem to be subjected to proteasome-mediated degradation (Fig. 2b).

AtMC9 was shown to cleave AtSerpin1 *in vitro* at the predicted cleavage site (R351, corresponding to the predicted reactive center loop of AtSerpin1) (Vercammen *et al.*, 2004). Similarly, we observed that AtSerpin1 was cleaved by AtMC1 (Fig. 3). This cleavage was partly dependent on an intact catalytic site, as the levels of the cleaved fragment were lower or not detectable when YFP-AtSerpin1 (Fig. S4b) or AtSerpin1-YFP (Figs 3, S4a) was coexpressed with AtMC1-CA. In this experimental system, endogenous *N. benthamiana* proteases, including metacaspases, may also have the capacity to cleave AtSerpin1 as indicated by the cleavage products that appear on the sample expressing AtSerpin1 alone (Fig. 3, lane 5).

AtSerpin1 colocalizes and coimmunoprecipitates with AtMC1

To assess whether AtSerpin1 and AtMC1 colocalize, we obtained fluorescently tagged versions of both proteins (AtSerpin1-GFP and AtMC1-RFP) and tested their subcellular localization under confocal laser scanning microscopy. As shown in Fig. 4, both proteins colocalize in the cytoplasm. In addition, AtSerpin-GFP, but not AtMC1, is visualized in the nucleus of *N. benthamiana* cells when transiently overexpressed, probably as the result of GFP cleavage.

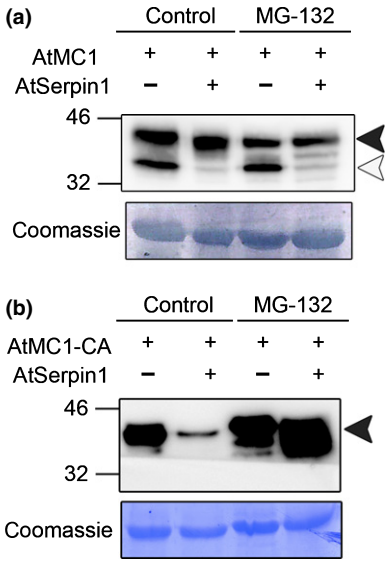

Fig. 2 AtSerpin1 inhibits AtMC1 autoprocessing and enhances proteasome-mediated degradation of the catalytic dead version of the protein (AtMC1-C220A). Wild-type and catalytic dead (CA) AtMC1-HA versions were transiently expressed in *Nicotiana benthamiana* leaves alone or in combination with *AtSerpin1-YFP*. Leaves were treated with 2 μM MG-132 (+) or left untreated (–). Proteins were extracted 12 h later and either Coomassie-stained or immunoblotted using anti-HA antibodies to detect, respectively, AtMC1-HA (a) or AtMC1-CA-HA (b). Black and white arrows indicate full-length and cleaved AtMC1, respectively.

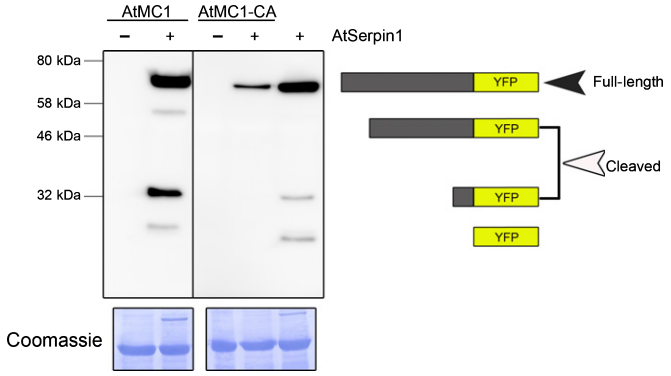

Fig. 3 AtSerpin1 is cleaved by AtMC1. *AtSerpin1-YFP* alone or in combination with *AtMC1-HA* or *AtMC1-CA-HA* was transiently expressed in *Nicotiana benthamiana* leaves. Total proteins were extracted and 50 μg were either Coomassie-stained or immunoblotted using anti-GFP antibody. The black arrowhead indicates full-length AtSerpin1, whereas the white arrowhead points at the putative AtSerpin1 cleaved form. YFP, yellow fluorescent protein.

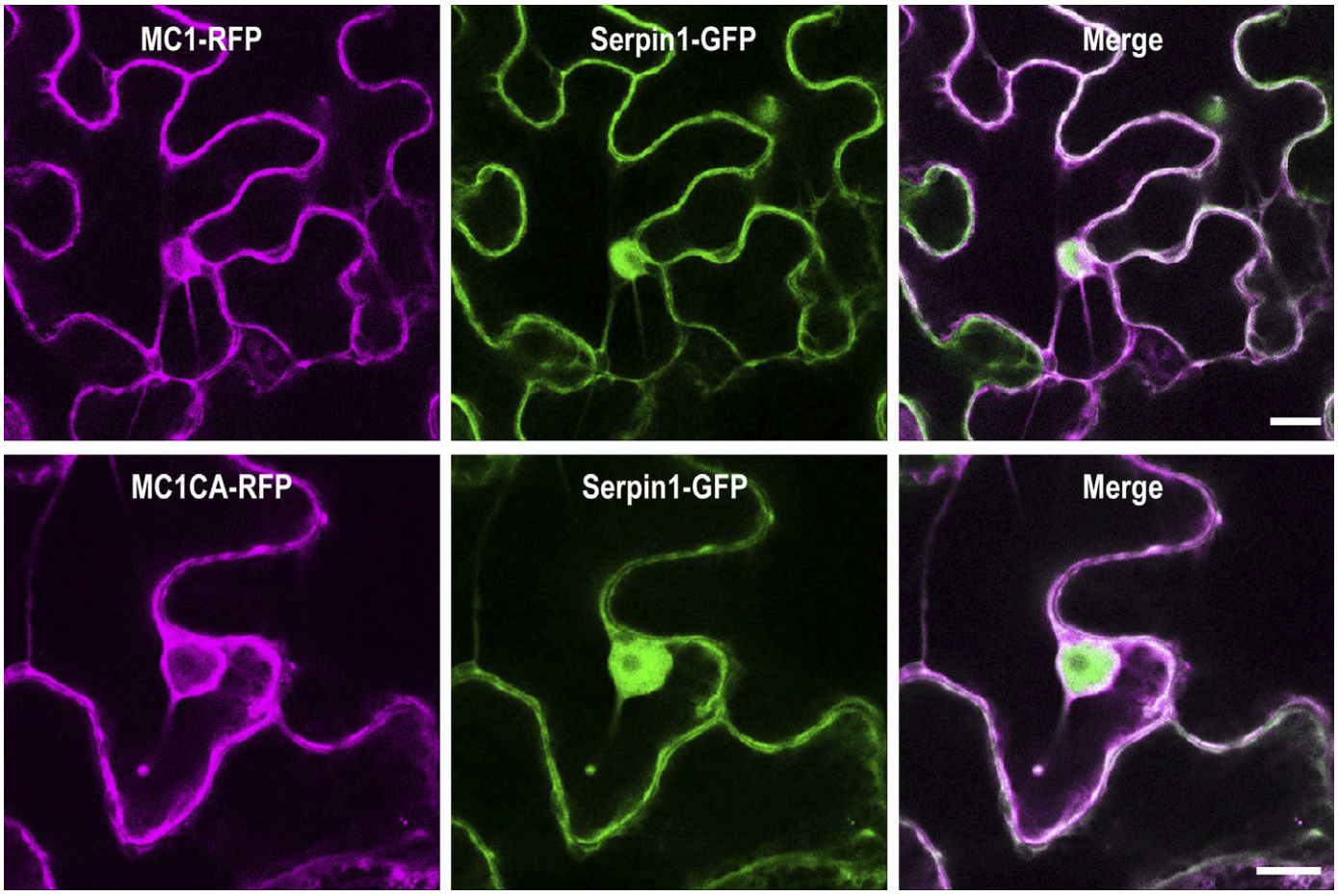

Fig. 4 Colocalization of AtSerpin1 and different forms of AtMC1. Confocal images of epidermal *Nicotiana benthamiana* cells 40 h after *Agrobacterium*-mediated transient expression of the indicated constructs. RFP, red fluorescent protein; GFP, green fluorescent protein. Bars, 15 μm.

Next, we analyzed whether AtMC1 and AtSerpin1 were able to form covalent complexes. For this, we performed protein extraction under nonreducing conditions in *N. benthamiana* plants expressing AtMC1-HA (*c.* 40 kDa) alone or in combination with AtSerpin1-YFP (*c.* 72 kDa). The observed molecular weight of 100 kDa, detected by both GFP and HA antibody, is consistent wth a noncanonical full-length serpin–protease complex (Figs 5, S5). This band is not present when using the reducing agent DTT in the extraction. The putative complex band also cannot be observed when, instead of wild-type AtMC1, the catalytic dead version of the protein AtMC1-CA is coexpressed together with AtSerpin1 in nonreducing conditions. This indicates that AtMC1–AtSerpin1 complex formation requires an AtMC1 intact catalytic site. Interestingly, the AtSerpin1-dependent degradation of AtMC1-CA seems to be lost under nonreducing conditions (Fig. 5). This could be a result of the stabilization of AtMC1 in an oxidizing environment.

To further specify the requirements of the AtMC1–AtSerpin1 noncanonical interplay, we performed coimmunoprecipitation experiments with AtSerpin1 and different AtMC1 forms. Total protein extracts from transiently expressed *AtMC1-HA* alone or together with *AtSerpin1-YFP* were incubated with magnetic beads coupled with anti-GFP antibody. Immunoblot of total protein and the eluted fraction confirmed AtMC1 and AtSerpin1 coimmunoprecipitation (Fig. 6a). We obtained the same result when using Arabidopsis double transgenic plants coexpressing *AtMC1* and *AtSerpin1* (Fig. S6). As expected, the catalytic dead version of the protein (AtMC1-CA) did not coimmunoprecipitate with AtSerpin1 when transiently coexpressed in *N. benthamiana* (Fig. 6b). This corroborates the fact that an intact AtMC1 catalytic site is required for coimmunoprecipitation.

To determine whether AtSerpin1 interacts with AtMC1 through its prodomain, we performed coimmunoprecipitation using a prodomain-less version of AtMC1 (AtMC1-ΔN-HA) (Coll *et al.*, 2010). As shown in Fig. 6(c) this is not the case, as AtMC1-ΔN-HA still coimmunoprecipitated with AtSerpin1, albeit to a lesser extent than the full-length version.

AtSerpin1 inhibits AtMC1-dependent programmed cell death

To address whether AtSerpin1 had an effect on AtMC1-mediated cell death, we carried out ion leakage analysis on *N. benthamiana* plants transiently expressing the different forms of *AtMC1* (*AtMC1*, *AtMC1-CA* and *AtMC1-ΔN*) alone or in combination with *AtSerpin1* (Fig. 7a,b). As expected, *AtMC1* expression

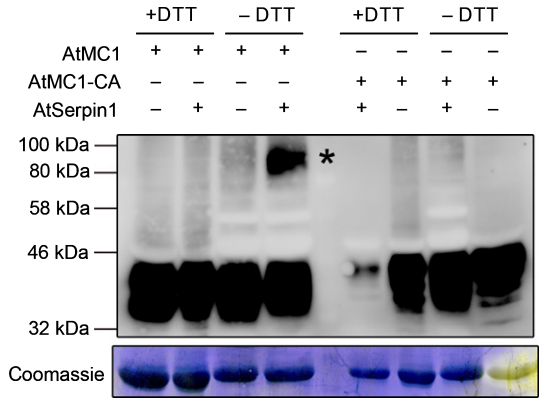

Fig. 5 Binding between AtMC1 and AtSerpin1 occurs only in presence of an intact catalytic site. Full-length *AtMC1-HA* and *AtMC1-CA-HA* were transiently expressed in *Nicotiana benthamiana* leaves alone or in combination with *AtSerpin1-YFP*. Total proteins were extracted under reducing (+DTT) or nonreducing (−DTT) conditions. Fifty micrograms of protein were separated on a sodium dodecyl sulfate–polyacrylamide gel electrophoresis and either Coomassie-stained or immunoblotted using anti-HA antibody. The asterisk indicates the putative *AtMC1-AtSerpin1* complex.

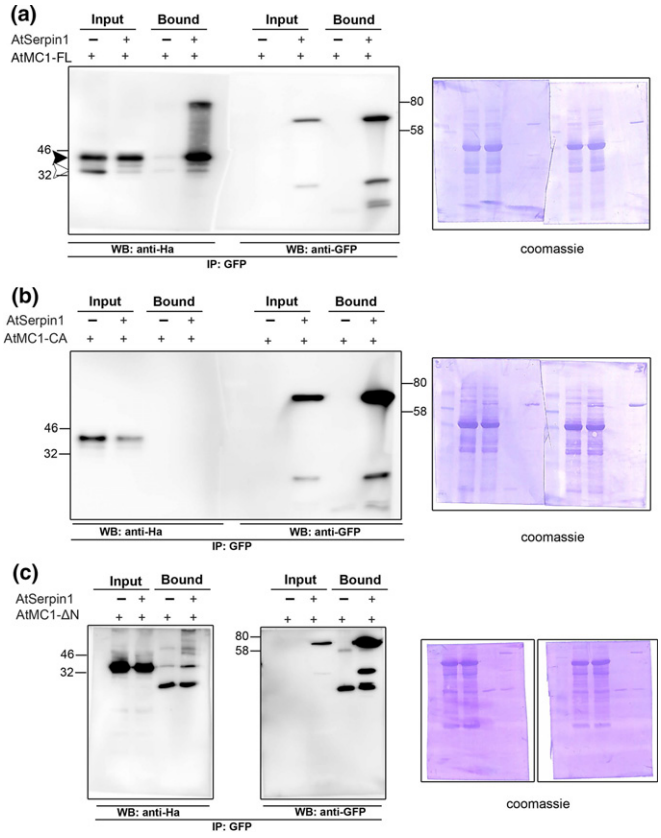

Fig. 6 AtMC1-AtSerpin1 coimmunoprecipitation occurs independently of AtMC1 prodomain but an intact catalytic center is required. Different *AtMC1-HA* forms (FL, full length; CA, catalytic dead; ΔN, prodomain-less) were transiently expressed in *Nicotiana benthamiana* leaves alone or in combination with *AtSerpin1-YFP*. Total proteins were extracted (input), incubated with magnetic beads coupled to green fluorescent protein (GFP) And, after stringent washes, proteins bound to the beads were eluted (bound). Input and bound fractions were either Coomassie-stained or probed against anti-GFP to detect AtSerpin or against anti-HA to detect AtMC1-FL (a), AtMC1-CA (b) or AtMC1-ΔN (c). The black arrowhead indicates full-length AtMC1, whereas the white arrowhead points at the putative AtMC1 cleaved form. WB, western blot; IP, immunoprecipitation. [Correction added after online publication 3 February 2017: the duplicated anti-GFP immunoblot in (a) has been replaced with the correct immunoblot and the Coomassie-stained panels in (a) and (b) have been switched to match their immunoblots. For clarity full images of all gels and Coomassies are now shown.]

caused an increase in ectopic cell death over time. This cell death was also observed when expressing the ΔN form of the protein and was almost completely abolished in leaves expressing the catalytic dead version of *AtMC1* (*AtMC1-CA*). AtSerpin1 clearly blocked AtMC1- and AtMC1-ΔN-dependent cell death, further supporting the idea that it acts as a bona fide inhibitor of AtMC1 activity.

In order to genetically substantiate this claim, we monitored cell death on *atmc1*, *atserpin1* and *atmc1 atserpin1* mutant plants and plants overexpressing *AtSerpin1* (AtSerpin1-HA) compared with the wild-type. As a cell death trigger, we used *Pseudomonas syringae* pv tomato expressing the type III effector *avrRpm1* (*Pto* DC3000(*avrRpm1*)), which causes AtMC1-dependent HR cell death mediated by the RPM1 receptor (Coll *et al.*, 2010). Two-week-old plants were infected with *Pto* DC3000(*avrRpm1*) and cell death was quantified using a single cell death assay (Coll *et al.*, 2010, 2014). As previously observed, the lack of *atmc1* resulted in a sharp decrease in RPM1-mediated cell death (Fig. 7c). Double *atmc1 atserpin1* mutants showed reduced cell death levels, lower than the wild-type but higher than *atmc1* plants, whereas *atserpin1* mutants behaved similarly to the wild-type. Together, these data suggests that AtSerpin1 acts as a negative regulator of cell death mediated by AtMC1 via (an) additional protease(s) in Arabidopsis.

Discussion

AtMC1 is an autocatalytically active protease *in planta*

In the past we speculated that AtMC1 and the animal inflammatory caspase-1, may share certain functional similarities (Coll *et al.*, 2010, 2014). This was based on the following facts: analogous catalytic domain structure; both are positive regulators of cell death induced upon immune receptor activation; presence of a prodomain that contains cell death-related motifs; and both are negatively regulated by an inactive member of their family (caspase-11 in the case of caspase-1 and AtMC2 in the case of AtMC1).

In animals, the caspase-1-dependent response is very well characterized (Davis *et al.*, 2011). Upon immune receptor activation, supramolecular structures termed inflammasomes are assembled, recruiting multiple copies of full-length, inactive caspase-1. Within inflammasomes, many caspase-1 units are rapidly self-processed through induced proximity, releasing p10 and p20 subunits that then assemble into the active form, consisting of two p20–p10 heterodimers. Active caspase-1 can then carry out multiple processes in response to the initial inflammatory signal, generating a fast and efficient response.

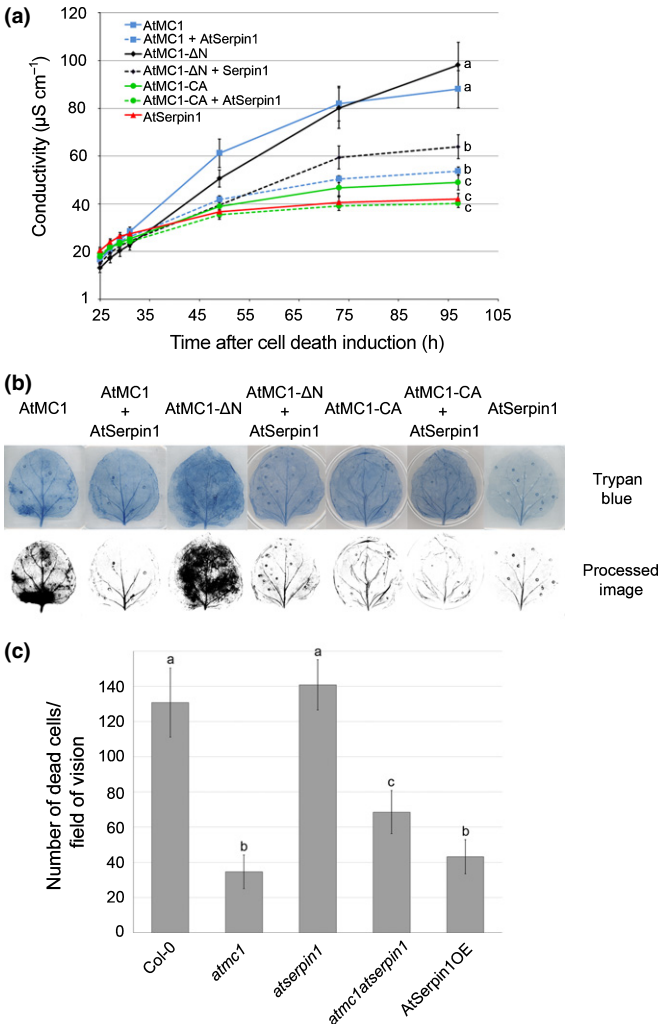

Fig. 7 AtSerpin1 inhibits AtMC1-mediated cell death. (a) Ion leakage assay using *Nicotiana benthamiana* leaves expressing the different forms of *AtMC1-HA* alone or in combination with *AtSerpin1-YFP*. Cell death was induced by dexamethasone treatment 48 h after agroinfiltration of the leaves (time 0). Each time point corresponds to the SE of six replicates containing 10 leaf disks each ($\pm 2 \times$ SE). Letters indicate significant differences following post-ANOVA Tukey's honest significant difference test ($\alpha = 0.05$). This experiment was repeated five times with similar results. (b) Pictures of representative trypan blue-stained leaves expressing the different forms of *AtMC1* alone or in combination with *AtSerpin1* 72 h after cell death induction (upper row) or the same images processed using Image J to highlight dead areas (lower row). (c) Single cell death assay of the indicated *Arabidopsis thaliana* lines. Dead cells (trypan blue-positive) were counted under an optical microscope 12 h after infection with 250 000 colony-forming units ml^{-1} *Pto* DC3000(*avrRpm1*). Values indicate the average of 50 samples per genotype $\pm 2 \times$ SE. Letters indicate significant differences following post-ANOVA Tukey's honest significant difference test ($\alpha = 0.05$). The experiment is representative of five independent replicates.

Our data support the idea that AtMC1 is catalytically self-processed to release the prodomain and a fragment encompassing the p20 and p10 subunits. Several other type I metacaspases have been shown to self-cleave (Meslin *et al.*, 2007; Moss *et al.*, 2007; Zalila *et al.*, 2011; Li *et al.*, 2015). However, the link between cleavage and activation has not yet been established. In fact, for the *Trypanosoma brucei* metacaspase TbMCA2, it was shown that cleavage is not critical for activation (Moss *et al.*, 2007). In Arabidopsis, AtMC1 appears to be maintained in an equipoise between the full-length and the processed form. Conditional overexpression of the processed form caused faster and more extensive cell death than the full-length version of AtMC1 (Coll *et al.*, 2010). This was in agreement with the idea that the prodomain is a negative regulator of type I metacaspase activity and might act as a physical barrier for substrate access (McLuskey *et al.*, 2012). However, we did not find any stress condition that increased the accumulation of the processed form (data not shown). This might imply that AtMC1 activation does not occur via enhanced processing but rather by relocalization of the prodomain-less form to a different subcellular compartment where relevant substrates are located or by post-translational modifications.

In fact, we still do not know whether AtMC1 or other type I metacaspases are recruited to death-induced supramolecular structures comparable to the inflammasome through their prodomain. Interestingly, the two metacaspase crystal structures resolved to date indicate that homodimerization through the equivalent interfaces as observed in caspases seem impossible (McLuskey *et al.*, 2012; Wong *et al.*, 2012). Thus, it remains an open question how AtMC1 and other metacaspases become active.

The interplay between AtSerpin1 and AtMC1 in plants

In the context of AtMC1 regulation, mechanisms to prevent its activation under homeostatic conditions must be in place to avoid unrestrained cell death propagation. Two negative regulators of AtMC1 function were identified earlier: AtMC2 and LSD1 (Coll *et al.*, 2010). Here, we have uncovered a novel negative regulator of AtMC1: the protease inhibitor AtSerpin1, which can block AtMC1 autocatalytic activity *in planta* and prevent AtMC1-mediated cell death.

Serpins are a superfamily of proteins, initially described as serine protease inhibitors, but now known to include cysteine protease inhibitors and even noninhibitory members (Gettins, 2002). Serpins are the most widespread and abundant peptidase inhibitors, being present in all domains of life and even in viruses (Rawlings *et al.*, 2004). In animals, serpins have been involved in cell survival, development and host defense against pathogens (Silverman *et al.*, 2010). Inhibitory serpins have been termed 'suicide inhibitors' or 'molecular mousetraps' because of their mode of action: cleavage by the target protease sets off a conformational change in the serpin whereby the protease is flipped and becomes trapped against the serpin protein body, with its catalytic core crushed and the consequent decrease in proteolytic activity (Huntington *et al.*, 2000).

The Arabidopsis genome encodes eight serpin genes (Fluhr *et al.*, 2012). Among them, the most abundant and best characterized is *AtSerpin1*. The *in vitro* proteolytic activities of two type II metacaspases, AtMC4 and AtMC9, were shown to be inhibited by AtSerpin1 (Vercammen *et al.*, 2004). In turn, AtMC9 was demonstrated to cleave AtSerpin1 *in vitro* at the predicted

cleavage site (reactive center loop) in a dose-dependent manner (Vercammen *et al.*, 2004). Our *in vivo* data indicate that AtMC1 might also be able to cleave AtSerpin1 through its reactive center loop, as the size of two fragments generated would be in agreement with the corresponding prediction.

Both AtMC4 and AtMC9 were shown to act as positive regulators of cell death in different contexts: AtMC4 was involved in pathogen-triggered cell death (Watanabe & Lam, 2011), whereas AtMC9 participates in developmental cell death, mediating cell clearance in late stages of xylem formation (Bollhoner *et al.*, 2013). In neither case has it been established that inhibition of AtMC activity by AtSerpin1 affects metacaspase function in these physiological contexts.

Here, we demonstrated inhibition of AtMC1 by AtSerpin1 *in vivo*. This inhibition was monitored as loss of self-processing of AtMC1 when coexpressed with AtSerpin1. Unfortunately, we have so far not been able to directly measure AtMC1 proteolytic activity, and thus we have not been able to assess the effect of AtSerpin1 on it. We also observed that AtMC1-CA was partly degraded by the proteasome and coexpression with AtSerpin1 dramatically exacerbated AtMC1-CA proteasomal degradation. AtMC1-CA is more prone to aggregation than its wild-type counterpart (Coll *et al.*, 2014) and cells have evolved different surveillance mechanisms to detect and eliminate potentially toxic protein aggregates. Thus, it is not surprising that at least part of the AtMC1-CA pool is delivered to the proteasome for degradation. The fact that AtSerpin1 coexpression enhances AtMC1-CA proteasome-mediated degradation could indicate that AtSerpin1 might interact and/or induce a conformational change in AtMC1-CA that further promotes its aggregation and, consequently, its elimination via the proteasome.

AtMC1 and AtSerpin1 colocalize and coimmunoprecipitate, indicating a possible interaction between the two proteins. In contrast to the previously shown AtMC1-LSD1 coimmunoprecipitation (Coll *et al.*, 2010), the prodomain was not required for the interaction between AtMC1 and AtSerpin. The interaction between AtMC1-ΔN and AtSerpin1 still took place, although it was weaker than with the full-length version of AtMC1, indicating a less stable interaction when the prodomain was missing. However, an intact AtMC1 catalytic center was required for the coimmunoprecipitation. This was presumably not the case for AtMC9-AtSerpin1 interaction, as a catalytic-dead version of AtMC9 was used as a bait for AtSerpin1 identification in the yeast two-hybrid assay (Vercammen *et al.*, 2006). The apparent discrepancy of the two observations might be explained by a weaker affinity between AtSerpin1 and catalytic-dead metacaspase mutants. These potentially weak interactions are probably eliminated by the stringent washes of a coimmunoprecipitation experiment, whereas they remain intact in yeast two-hybrid assays.

AtSerpin1 as an inhibitor of cell death proteases

In plants, AtSerpin1 might act as a pan-metacaspase inhibitor or even as a more general cell death protease inhibitor. AtSerpin1 was shown to covalently bind and to modulate the activity of the cell death protease RD21 (Lampl *et al.*, 2010, 2013). Our data also indicate that AtSerpin1 forms a noncanonical complex with AtMC1, detected under nonreducing conditions. This discrepancy between the mode of interaction between different metacaspases and AtSerpin1 could be a result of the different mode of action of AtMC1 and 9, their localization (subcellular and tissular) and the processes in which they are involved.

Interestingly, the interplay between AtMC1 and AtSerpin1 seem to involve the full-length rather than the cleaved versions of the proteins. Although AtMC1 may be able to cleave AtSerpin1, the size of the complex detected, as well as the coimmunoprecipitated fragments indicate a noncanonical mode of action whereby AtSerpin1 would bind and inactivate AtMC1 but this interaction would not involve self-cleavage or direct AtSerpin1 cleavage by AtMC1. The fact that AtMC1 catalytic activity is required for the interaction with AtSerpin1 could suggest the involvement of a third partner that needs to be cleaved in order for the inhibition to take place or nondetectable modifications of AtMC1 and/or AtSerpin1.

Overexpression of *AtSerpin1* or a mutation in the protease RD21 led to reduced cell death after infection with the necrotrophic fungi *Botrytis cinerea* and *Sclerotina sclerotiorum* but enhanced cell death in response to the hemibiotrophic fungus *Colletotrichum higgisianum* (Lampl *et al.*, 2013). In our conditions, infection with *Pto* DC3000(*avrRpm1*), a hemibiotrophic bacterium that causes HR in *A. thaliana* Col-0 background via the RPM1 receptor, resulted in decreased cell death in plants overexpressing *AtSerpin1*, comparable to *atmc1* mutants. Double *atmc1 atserpin1* mutants displayed an intermediate phenotype between wild-type and *atmc1* plants, which indicates that AtMC1 is negatively regulated by AtSerpin1 and also that *atserpin1* may control other proteases involved in this cell death process beyond *atmc1*. Whether AtSerpin1 inhibits AtMC1-regulated processes by directly interacting with AtMC1 or indirectly by modulating the activity of downstream proteases induced by AtMC1 remains an open question. Inhibition of AtMC1-mediated cell death by AtSerpin1 is also demonstrated by the dramatic effect of AtSerpin1 when transiently coexpressed with death-inducing forms of AtMC1 in *N. benthamiana* leaves. Discrepancy of results between *C. higgisianum* (Lampl *et al.*, 2013) and *Pto*, may be explained by the fact that, despite both being hemibiotrophs, their lifestyle, time and mode of infection are radically different and thus it is difficult to compare cell death outcomes at a given time point.

Inhibition of different cell death proteases by AtSerpin1 (Fig. S7) positions it as a conceivable guardian of cell homeostasis, preventing uncontrolled proteolysis of potentially dangerous proteins. The balance between the levels of AtSerpin1 and the levels of potentially active death proteases might be a powerful modulator of cell fate. Under normal conditions, molecule-by-molecule inactivation may serve as an effective surveillance mechanism that prevents uncontrolled cell death.

In animals, intracellular serpins have been shown to be major regulators of cell death and inflammation and this function partly occurs through direct inhibition of specific proteases, including caspases (Silverman *et al.*, 2010). Interestingly, this mechanism has been coopted by certain viruses, which are able to produce serpins in their hosts that block defenses (Gettins, 2002). For

example, the viral serpin CrmA efficiently inhibits caspase-1, escaping immune surveillance by the host (Ray *et al.*, 1992). In fact, in many species, lack of certain serpins results in severe phenotypes or cell death (Silverman *et al.*, 2010). The fact that *atserpin1* mutants have no dramatic phenotypes might be explained by the genetic redundancy within the serpin family in Arabidopsis, but more experimental evidence is needed to confirm this hypothesis.

The work presented here contributes to a better understanding of cell death control in plants. We have demonstrated that AtSerpin1 acts *in vivo* as an inhibitor of AtMC1-mediated cell death, emerging as a potential inhibitor of cell death proteases in plants. These results are of major evolutionary significance, as they indicate a conserved function of a protease inhibitor on cell death regulators from different kingdoms with unrelated mode of action (i.e. caspases vs metacaspases).

Acknowledgements

The authors would like to kindly thank Marc Planas, Simon Stael, Guy Salvesen, Vera Bonardi and Ignacio Rubio-Somoza for helpful comments. We thank David Smalley and Nedyalka Dicheva from the University of North Carolina Michael Hooker Proteomics Center for technical assistance with protein identification. Anouk Brackenier, Dominique Eeckhout and Geert De Jaeger from Ghent University and the Flanders Institute of Biotechnology (VIB) are thanked for sharing and helping to analyze the TAP results. Thanks to Robert Fluhr for sharing transgenic AtSerpin-HA seeds and anti-Serpin antibody, and to Roger Innes for kindly providing Gateway vectors for colocalization studies. This work was funded by projects AGL2013-46898-R (MINECO, Spain) to N.S.C. and M.V., EU-Marie Curie Actions (PCDMC-321738 and PIIF-331392) and BP_B 00030 from the Catalan Government to N.S.C.; S.L.A. holds a fellowship Convocatoria Abierta 2013 Primera Fase (grant agreement no. AR2Q4017) from SENESCYT, Ecuador; J.L.D. is an Investigator of the Howard Hughes Medical Institute, supported by the HHMI and the Gordon and Betty Moore Foundation (GBMF3030); I.S. is supported by an AgreenSkills fellowship within the EU Marie-Curie FP7 COFUND People Programme (grant agreement no. 267196); S.R. is supported by the French Laboratory of Excellence project 'TULIP' (ANR-10-LABX-41; ANR-11-IDEX-0002-02). We acknowledge financial support from the Spanish Ministry of Economy and Competitiveness, through the 'Severo Ochoa Programme for Centres of Excellence in R&D 2016-2019 (SEV-2015-0533)'.

Author contributions

S.L.A. performed and designed experiments, analyzed data and wrote the manuscript. D.V. performed and designed experiments and analyzed data. I.S. performed experiments and analyzed data. M.V. designed experiments and analyzed data. S.R. designed experiments, analyzed data and wrote the manuscript. F.v.B. designed experiments, analyzed data and wrote the manuscript. F.L.C. designed experiments, analyzed data and wrote the manuscript. J.L.D. designed experiments, analyzed data and wrote the manuscript. N.S.C. designed the research, performed experiments, analyzed data and wrote the manuscript. All authors reviewed the manuscript.

References

Aravind L, Koonin EV. 2002. Classification of the caspase-hemoglobinase fold: detection of new families and implications for the origin of the eukaryotic separins. *Proteins* **46**: 355–367.

Bollhoner B, Zhang B, Stael S, Denance N, Overmyer K, Goffner D, Van Breusegem F, Tuominen H. 2013. Post mortem function of AtMC9 in xylem vessel elements. *New Phytologist* **200**: 498–510.

Campbell RE, Tour O, Palmer AE, Steinbach PA, Baird GS, Zacharias DA, Tsien RY. 2002. A monomeric red fluorescent protein. *Proceedings of the National Academy of Sciences, USA* **99**: 7877–7882.

Clough SJ, Bent AF. 1998. Floral dip: a simplified method for Agrobacterium-mediated transformation of *Arabidopsis thaliana*. *Plant Journal* **16**: 735–743.

Coll NS, Smidler A, Puigvert M, Popa C, Valls M, Dangl JL. 2014. The plant metacaspase AtMC1 in pathogen-triggered programmed cell death and aging: functional linkage with autophagy. *Cell Death and Differentiation* **21**: 1399–1408.

Coll NS, Vercammen D, Smidler A, Clover C, Van Breusegem F, Dangl JL, Epple P. 2010. Arabidopsis type I metacaspases control cell death. *Science* **330**: 1393–1397.

Cormack BP, Valdivia RH, Falkow S. 1996. FACS-optimized mutants of the green fluorescent protein (GFP). *Gene* **173**: 33–38.

Davis BK, Wen H, Ting JP. 2011. The inflammasome NLRs in immunity, inflammation, and associated diseases. *Annual Review of Immunology* **29**: 707–735.

Dietrich RA, Delaney TP, Uknes SJ, Ward ER, Ryals JA, Dangl JL. 1994. Arabidopsis mutants simulating disease resistance response. *Cell* **77**: 565–577.

Earley KW, Haag JR, Pontes O, Opper K, Juehne T, Song K, Pikaard CS. 2006. Gateway-compatible vectors for plant functional genomics and proteomics. *Plant Journal* **45**: 616–629.

Fluhr R, Lampl N, Roberts TH. 2012. Serpin protease inhibitors in plant biology. *Physiologia Plantarum* **145**: 95–102.

Gettins PG. 2002. Serpin structure, mechanism, and function. *Chemical Reviews* **102**: 4751–4804.

Gu Y, Innes RW. 2011. The KEEP ON GOING protein of Arabidopsis recruits the ENHANCED DISEASE RESISTANCE1 protein to trans-Golgi network/early endosome vesicles. *Plant Physiology* **155**: 1827–1838.

Huntington JA, Read RJ, Carrell RW. 2000. Structure of a serpin–protease complex shows inhibition by deformation. *Nature* **407**: 923–926.

Kaltenbrun E, Greco TM, Slagle CE, Kennedy LM, Li T, Cristea IM, Conlon FL. 2013. A Gro/TLE-NuRD corepressor complex facilitates Tbx20-dependent transcriptional repression. *Journal of Proteome Research* **12**: 5395–5409.

Keller A, Nesvizhskii AI, Kolker E, Aebersold R. 2002. Empirical statistical model to estimate the accuracy of peptide identifications made by MS/MS and database search. *Analytical Chemistry* **74**: 5383–5392.

Keogh RC, Deverall BJ, McLeod S. 1980. Comparison of histological and physiological responses to *Phakopsora pachyrhizi* in resistant and susceptible soybean. *Transactions of the British Mycological Society* **74**: 329–333.

Lampl N, Alkan N, Davydov O, Fluhr R. 2013. Set-point control of RD21 protease activity by AtSerpin1 controls cell death in Arabidopsis. *Plant Journal* **74**: 498–510.

Lampl N, Budai-Hadrian O, Davydov O, Joss TV, Harrop SJ, Curmi PM, Roberts TH, Fluhr R. 2010. Arabidopsis AtSerpin1, crystal structure and *in vivo* interaction with its target protease RESPONSIVE TO DESICCATION-21 (RD21). *Journal of Biological Chemistry* **285**: 13550–13560.

Li M, Wang H, Liu J, Hao P, Ma L, Liu Q. 2015. The apoptotic role of metacaspase in *Toxoplasma gondii*. *Frontiers in Microbiology* **6**: 1560.

McLuskey K, Rudolf J, Proto WR, Isaacs NW, Coombs GH, Moss CX, Mottram JC. 2012. Crystal structure of a *Trypanosoma brucei* metacaspase. *Proceedings of the National Academy of Sciences, USA* **109**: 7469–7474.

Meslin B, Barnadas C, Boni V, Latour C, De Monbrison F, Kaiser K, Picot S. 2007. Features of apoptosis in *Plasmodium falciparum* erythrocytic stage through a putative role of PfMCA1 metacaspase-like protein. *Journal of Infectious Diseases* **195**: 1852–1859.

Moss CX, Westrop GD, Juliano L, Coombs GH, Mottram JC. 2007. Metacaspase 2 of *Trypanosoma brucei* is a calcium-dependent cysteine peptidase active without processing. *FEBS Letters* **581**: 5635–5639.

Nakagawa T, Kurose T, Hino T, Tanaka K, Kawamukai M, Niwa Y, Toyooka K, Matsuoka K, Jinbo T, Kimura T. 2007. Development of series of gateway binary vectors, pGWBs, for realizing efficient construction of fusion genes for plant transformation. *Journal of Bioscience and Bioengineering* **104**: 34–41.

Nakamura S, Mano S, Tanaka Y, Ohnishi M, Nakamori C, Araki M, Niwa T, Nishimura M, Kaminaka H, Nakagawa T *et al.* 2010. Gateway binary vectors with the bialaphos resistance gene, bar, as a selection marker for plant transformation. *Bioscience, Biotechnology, and Biochemistry* **74**: 1315–1319.

Rawlings ND, Tolle DP, Barrett AJ. 2004. Evolutionary families of peptidase inhibitors. *Biochemical Journal* **378**: 705–716.

Ray CA, Black RA, Kronheim SR, Greenstreet TA, Sleath PR, Salvesen GS, Pickup DJ. 1992. Viral inhibition of inflammation: cowpox virus encodes an inhibitor of the interleukin-1β converting enzyme. *Cell* **69**: 597–604.

Roberts TH, Ahn JW, Lampl N, Fluhr R. 2011. Plants and the study of serpin biology. *Methods in Enzymology* **499**: 347–366.

Salvesen GS, Hempel A, Coll NS. 2016. Protease signaling in animal and plant-regulated cell death. *FEBS Journal* **283**: 2577–2598.

Silverman GA, Whisstock JC, Bottomley SP, Huntington JA, Kaiserman D, Luke CJ, Pak SC, Reichhart JM, Bird PI. 2010. Serpins flex their muscle: I. Putting the clamps on proteolysis in diverse biological systems. *Journal of Biological Chemistry* **285**: 24299–24305.

Tsiatsiani L, Van Breusegem F, Gallois P, Zavialov A, Lam E, Bozhkov PV. 2011. Metacaspases. *Cell Death and Differentiation* **18**: 1279–1288.

Uren AG, O'Rourke K, Aravind LA, Pisabarro MT, Seshagiri S, Koonin EV, Dixit VM. 2000. Identification of paracaspases and metacaspases: two ancient families of caspase-like proteins, one of which plays a key role in MALT lymphoma. *Molecular Cell* **6**: 961–967.

Vercammen D, Belenghi B, van de Cotte B, Beunens T, Gavigan JA, De Rycke R, Brackenier A, Inze D, Harris JL, Van Breusegem F. 2006. Serpin1 of *Arabidopsis thaliana* is a suicide inhibitor for metacaspase 9. *Journal of Molecular Biology* **364**: 625–636.

Vercammen D, van de Cotte B, De Jaeger G, Eeckhout D, Casteels P, Vandepoele K, Vandenberghe I, Van Beeumen J, Inze D, Van Breusegem F. 2004. Type II metacaspases Atmc4 and Atmc9 of *Arabidopsis thaliana* cleave substrates after arginine and lysine. *Journal of Biological Chemistry* **279**: 45329–45336.

Vinatzer BA, Teitzel GM, Lee MW, Jelenska J, Hotton S, Fairfax K, Jenrette J, Greenberg JT. 2006. The type III effector repertoire of *Pseudomonas syringae* pv. syringae B728a and its role in survival and disease on host and non-host plants. *Molecular Microbiology* **62**: 26–44.

Voinnet O, Rivas S, Mestre P, Baulcombe D. 2003. An enhanced transient expression system in plants based on suppression of gene silencing by the p19 protein of tomato bushy stunt virus. *Plant Journal* **33**: 949–956.

Watanabe N, Lam E. 2011. Arabidopsis metacaspase 2d is a positive mediator of cell death induced during biotic and abiotic stresses. *Plant Journal* **66**: 969–982.

Wong AH, Yan C, Shi Y. 2012. Crystal structure of the yeast metacaspase Yca1. *Journal of Biological Chemistry* **287**: 29251–29259.

Wroblewski T, Tomczak A, Michelmore R. 2005. Optimization of Agrobacterium-mediated transient assays of gene expression in lettuce, tomato and Arabidopsis. *Plant Biotechnology Journal* **3**: 259–273.

Wrzaczek M, Vainonen JP, Stael S, Tsiatsiani L, Help-Rinta-Rahko H, Gauthier A, Kaufholdt D, Bollhoner B, Lamminmaki A, Staes A *et al.* 2015. GRIM REAPER peptide binds to receptor kinase PRK5 to trigger cell death in Arabidopsis. *EMBO Journal* **34**: 55–66.

Zalila H, Gonzalez IJ, El-Fadili AK, Delgado MB, Desponds C, Schaff C, Fasel N. 2011. Processing of metacaspase into a cytoplasmic catalytic domain mediating cell death in *Leishmania major*. *Molecular Microbiology* **79**: 222–239.

Supporting Information

Additional Supporting Information may be found online in the Supporting Information tab for this article:

Fig. S1 Schematic representation of all constructs used in this study.

Fig. S2 Immunoprecipitation of AtMC1 native form in *Arabidopsis thaliana*.

Fig. S3 Comparison of AtMC1 expression levels when expressed under native vs dexamethasone-inducible promoter.

Fig. S4 Binding between AtMC1 and AtSerpin1.

Fig. S5 AtMC1 and AtSerpin1 co-immunoprecipitate in *Arabidopsis thaliana*.

Fig. S6 AtSerpin1 is cleaved by AtMC1.

Fig. S7 AtSerpin1, an inhibitor of cell death proteases in plants.

Table S1 Identification of AtMC1 and AtSerpin1 by LC-MS/MS after HA immunoaffinity purification

Table S2 Identification of AtMC1 and AtSerpin1 by LC-MS/MS after TAP purification

Please note: Wiley Blackwell are not responsible for the content or functionality of any Supporting Information supplied by the authors. Any queries (other than missing material) should be directed to the *New Phytologist* Central Office.